RSC Advances

PAPER

View Article Online
View Journal | View Issue

Cite this: *RSC Adv.*, 2022, **12**, 18646

Feasibility study on further enhanced oil recovery by ISC of remaining oil after polymer flooding

Fajun Zhao, *[a] Guangmeng Zhu,[a] Guo Li,[b] Yifan Jiang[a] and Lei Liu[a]

The residual oil after polymer flooding in China is highly dispersed. The reservoir's interlayer and intralayer contradictions are prominent, the polymer flooding efficiency is significantly reduced, and the exploitation difficulty is increased. An indoor physical simulation experiment of undertaking fire flooding after polymer flooding is conducted to investigate the recovery measures that can undertake polymer flooding and further improve the recovery degree of residual oil. The stability of the combustion front and the basic parameters of *in situ* combustion (ISC) were studied, and the crude oil properties before and after the fire flooding were analyzed. The results show that the temperature range and variation trend of the combustion front in the polymer flooding-to-fire flooding experiment are similar to those in the conventional fire flooding experiment. The combustion front advances steadily, indicating that the residual oil can be burned effectively after polymer flooding, providing an application basis for fire flooding. The calculated apparent H/C atomic ratio through the tail gas composition is 1.33, which further demonstrates that a high-temperature oxidation reaction occurs at the combustion front, and the displacement efficiency of the burned oil layer is 72.1%. A comparison of the oil samples before and after fire flooding shows that the carbon number of *n*-alkanes in the oil produced after fire flooding increases, improving the quality of crude oil.

Received 1st April 2022
Accepted 20th June 2022

DOI: 10.1039/d2ra02118h

rsc.li/rsc-advances

1 Introduction

Currently, the production of onshore thin oil reservoirs in China has been significantly improved after stimulation measures, such as polymer flooding. When the reservoir developed by polymer flooding enters the middle and later stages, the effect of polymer injection increasingly becomes worse, and the water content in the produced fluid increases. Maintaining economic and effective development with continuous polymer injections is difficult. However, a considerable amount of crude oil remains in the formation after polymer flooding. Therefore, replacement technology research has very far-reaching significance. *In situ* combustion (ISC) technology has various applications and is often used in primary or secondary oil production. It has proved relatively flawless as a mining technology for ordinary heavy oil and some extra-heavy oil reservoirs following years of research.

The two development methods of ISC and low-temperature oxidation of air injection are the two main branch technologies of air injection oil recovery.[1] These two technologies have different characteristics and mechanisms. The low-temperature oxidation technology of dilute oil injection air involves injecting air into the original reservoir, releasing a certain amount of heat through the low-temperature oxidation reaction to maintain and improve the reaction zone's temperature, causing the formation oil temperature to increase and viscosity to decrease, and effectively consuming oxygen to generate CO_2. The CO_2 dissolves in crude oil to improve the formation energy and further reduce the viscosity of the formation oil. Its development mechanism is a combination of a flue gas drive and partial thermal effect.[2–4] If low-temperature oxidation reactions do not consume all the oxygen in the formation, the oxygen concentration in the production well will reach 10%, posing safety risks.[5,6] The ISC involves the formation of a high-temperature combustion front with a temperature higher than 350 °C by artificial ignition to realize the combustion and heat release in the oil layer and push the crude oil from the gas injection well to the production well.[7,8] The ISC has a high recovery factor, good thermal efficiency, and several applications.[9–12] If the ISC is introduced into a light oil reservoir and oxygen is rapidly consumed using a high-temperature combustion front, it can solve the problem of oxygen safety in the light oil injection air on the one hand, and improve the crude oil recovery factor on the other hand.[13–28]

Therefore, the ISC technology can be used as a polymer-flooding technology replacement method to further improve oil recovery. However, studies on whether the ISC technology is suitable for thin oil reservoirs after polymer flooding are limited. Thus, the characteristics of the combustion parameters

[a]*Key Laboratory of Entered Oil Recovery of Education Ministry, Northeast Petroleum University, Daqing, Heilongjiang 163318, China. E-mail: fajzhao@126.com*
[b]*Petroleum Production Engineering Research Institute of PetroChina, Daqing Oilfield Company, Daqing, Heilongjiang, 163453, China*

of the thin oil after polymer flooding, the composition of the produced oil, and the compositional changes of the functional groups must be investigated. In this study, a one-dimensional combustion tube was used to simulate the experiment of ISC in a thin oil reservoir after polymer flooding. The combustion law can be investigated using combustion experiments, and the basic combustion parameters, such as fuel consumption, fuel apparent H/C atomic ratio, and oil displacement efficiency, can be clarified. The stability of the combustion process can also be assessed by the temperature of the combustion front.

2 Experimental section

2.1 Experimental apparatus and instruments

The physical simulation experimental system of ISC mainly includes a gas injection system, ignition system, model ontology, data acquisition system, output liquid–gas separation, and recovery system, and Fig. 1 shows a schematic of the one-dimensional physical simulation experimental setup of ISC. The model body has rotation function, and can carry out dry and wet burning oil reservoir simulation experiments under different formation conditions. There are 20 temperature sensors distributed along the axis. The electric heating rod is inserted near the side of the simulated gas injection well, and the ignition system is connected with the regulator and power supply. The ignition temperature is controlled by the ignition system during the experiment. The air injection system is composed of air compressor and flow meter, which can meet the needs of adjusting the air injection intensity in the experimental process, and realize the accurate measurement and control of the air injection rate. The data acquisition system composed of thermocouple, data acquisition board and computer can display and automatically record the temperature change of each temperature measurement point in the experimental process. The geometric dimensions of the model body is 120 cm × 8 cm, the maximum working pressure of the model is 10 MPa, the maximum working temperature is 1000 °C.

2.1.1 Experimental instruments. iS10 infrared spectroscopy (PerkinElmer, USA), 7890A gas chromatography (Agilent, USA), alumina adsorption chromatography column (Shenyang Glass Instrument Factory), JA2003N electronic balance (Shanghai Jingke Instrument), and one-dimensional fire-flooded experimental device (self-developed by Northeast Petroleum University).

2.2 Experimental preparation and method

2.2.1 Experimental materials. The experiments of polymer flooding, transferring fire flooding, and direct fire flooding were designed to investigate the temperature distribution and combustion characteristics of each zone in the combustion process after the polymer injection, as well as the effect of high water content in the reservoir after the polymer injection. The sand used for the experiment was quartz sand with particle size similar to that of the oil layer. The sand reflected the physical characteristics of the underground reservoir core. The selected crude oil was mixed with quartz sand and simulated formation water in a certain ratio to obtain artificial oil sand with the same oil and water saturation. The viscosity of crude oil is 62.0 mPa s

Table 1 Experimental material parameters

Type	Experimental parameters	Value
Crude oil	Density/(g cm^{-3})	0.8724
	Viscosity/mPa s (50 °C)	62.00
Experimental sand	Density/(g cm^{-3})	2.47

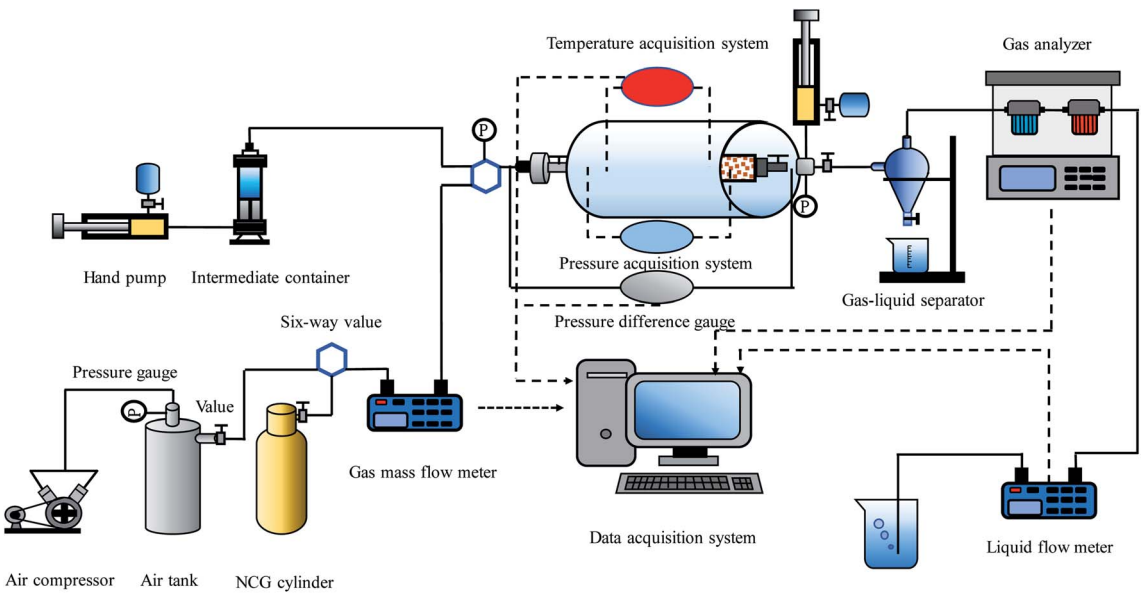

Fig. 1 Illustration of one-dimensional physical simulation experiment device for *in situ* combustion.

and its density is 0.8724 g cm^{-3}, and Table 1 shows the experimental material parameters.

2.2.2 Experimental conditions. Quartz sand that matches the reservoir core particles and reflects the reservoir's physical properties are used for filling. Table 2 shows the basic physical parameters and subsequent experimental conditions after filling.

2.3 Experimental procedure

(1) The prepared oil sands were loaded into the model; (2) model sealing, N_2 injection for connectivity test between injection and mining, and gas tightness test; (3) debugging the temperature acquisition system and establishing the initial temperature field in the process of N_2 injection, debugging the measurement and control system and preparing the connection of the output system; (4) starting the ignition and gas injection system, when the ignition temperature reaches 500 °C, the injected gas is changed from N_2 to air, and the physical simulation experiment of burning oil layer is carried out; (5) ventilation was continued even after the combustion was completed to bring the temperature of the model body down to room temperature.

2.4 Analytical test methods

The composition of the group in crude oil was determined using silica gel and alumina as adsorbents, and the results were compared with the standard. The saturated hydrocarbon, aromatic hydrocarbon, and nonhydrocarbon fractions were washed out, separated, and weighed to obtain the content of each component in the specimen using solvents of different polarities.

A 0.2–1.0 μL sample (which should be heated to no more than 50 °C and injected with an equal volume of CS_2 solvent) is extracted using a microsyringe and injected, while the program for temperature increase and chromatography is initiated, and the chromatogram and raw data are recorded.

Oil sand samples (about 1 mg) were thoroughly mixed with dried spectrally pure-grade KBr powder (about 100 mg) and ground in a dry environment with an agate mortar, finely mixed and transferred to a mold, put in a press bar, and then put on an oil press at a pressure of 10 t cm^{-2} for 5 min to obtain a transparent flake for infrared spectrum detection.

Table 2 Experimental condition

Number	Experimental parameters	ISC	ISC after polymer flooding
1	Ventilation intensity N $m^3/(m^2\ h)$	60.00	60.00
2	Permeability/μm^2	2.33	2.12
3	Porosity/%	31.85	32.94
4	Oil saturation/%	45.02	31.83
5	Water content saturation/%	54.98	68.17
6	Ignition temperature/°C	500.00	500.00
7	Pressure/MPa	5.00	5.00

3 Experimental results and analysis

3.1 Evaluation of combustion stability

3.1.1 Temperature field characteristics. Twenty thermocouples are evenly distributed along the one-dimensional combustion tube model. The temperature acquisition system records the temperature of each monitoring point along the combustion tube from the start of ignition to the end of combustion. The air is injected through a continuous heating igniter. The combustion front moves slowly to the production well after ignition. Fig. 2 and 3 show the temperature field distributions of the converted fire flooding experiment and the fire flooding experiment after polymer flooding, respectively. The maximum temperature of the combustion front of polymer flooding to fire flooding is 529.3 °C, while the minimum temperature is 331.6 °C. The fire line advances steadily. The maximum temperature of the combustion front of the fire flooding is 476.9 °C, while the minimum temperature is 350.6 °C. The comparison of the two figures shows that the trend of fire drive propulsion when oil saturation is 31.83% is

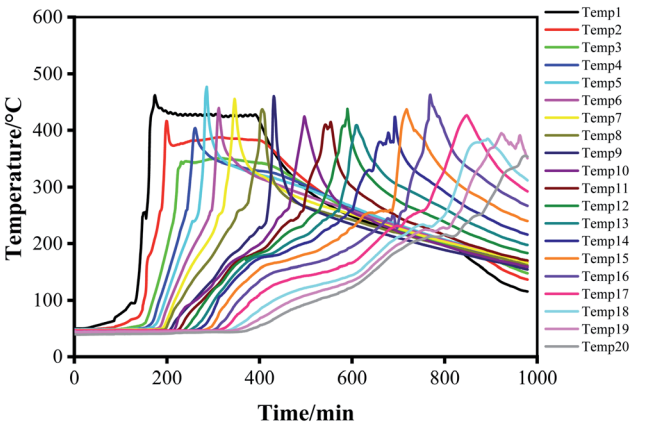

Fig. 2 Temperature curve of the combustion front during crude oil *in situ* combustion.

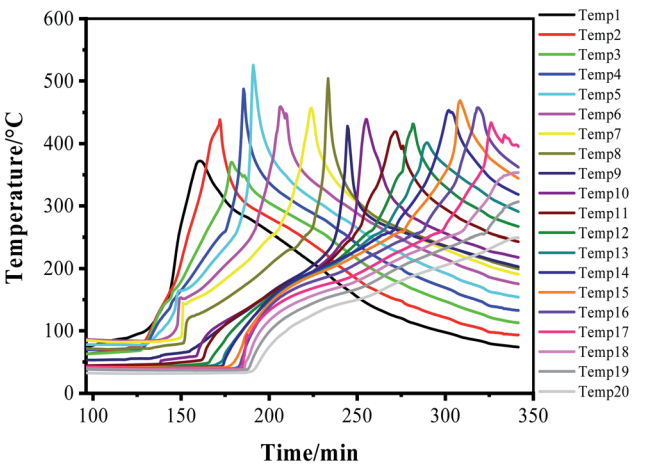

Fig. 3 Temperature curve of the residual oil combustion front after polymer flooding residual oil *in situ* combustion.

similar to that when oil saturation is 45.02%, and the maximum temperature of the combustion front is much higher than that of the latter when oil saturation is 31.83%, and the minimum temperature of the combustion front is just slightly lower. This shows that the fire flooding experiment after polymer flooding can effectively ignite and still has good combustion stability. The residual oil formation can sufficiently maintain combustion, and the fire flooding technology is feasible.

3.1.2 Determination of threshold temperature. The threshold temperature is the lowest ignition temperature that can ignite the oil sands in 1 h under continuous and constant air injection, and it is the most significant parameter for the design of heater power and heating duration in the ignition stage of the ISC of the oil field test. Several temperature measuring points are chosen in the model's center for data analysis. Fig. 4 and 5 show the relationship curve between the temperature change of the combustion front and its change rate with time. Before the oil sand is ignited, the oil sand is mainly heat-transferred by heat conduction, and the change in the oil sand temperature is relatively slow and stable. After the oil sand is ignited, the high-temperature oxidation of crude oil releases a large amount of heat, and the heat gathers in the local range of the combustion zone, resulting in a rapid increase in the temperature of the combustion front and a sharp increase in the temperature rise rate. The temperature gradually decreases as the fire line advances. Therefore, the maximum value of the heating rate is the moment of oil sand ignition. The threshold temperature can be obtained on the corresponding temperature–time curve, that is, the threshold temperature of crude oil fire flooding is 307.1 °C, and that of polymer flooding is 337.9 °C.

3.1.3 One-dimensional combustion-the tube exhaust-gas composition. A flue gas analyzer was used to monitor the contents of output flue gas components (CO, CO_2, and O_2) in real-time during the experiment, and the effluent gas content *versus* the time curve was obtained. Fig. 6 and 7 show the diagrams of fire flooding tail gas after polymer flooding and fire flooding tail gas, respectively. Fig. 6 shows that when the fire line was formed, the O_2 content decreased from 20.46% to about 6%, and CO and CO_2 were generated and increased rapidly, which were about 7% and 12%, respectively. Fig. 7 shows that when the fire line was formed, the O_2 content decreased from 21% to about 5%, and CO and CO_2 were generated and increased rapidly, which were about 8% and 13%, respectively. A comparison of the two figures shows that the curve changes in the figures are similar. The CO and CO_2 contents increase dramatically after the rapid decrease in O_2 content, and the contents of the three gases fluctuate up and down in a certain range. And O_2 content and CO, CO_2 content was negatively correlated, CO and CO_2 contents were positively correlated. A comparative analysis of the temperature field and effluent gas components during the fire flooding experiment showed that the temperature profile of the fire front of the residual oil after polymer flooding was similar to the trend of the fire front temperature profile of crude oil, normal heavy oil, extra-heavy oil, and super heavy oil.[25,26] Thus, the fire flooding of the residual oil after the polymer flooding can guarantee the

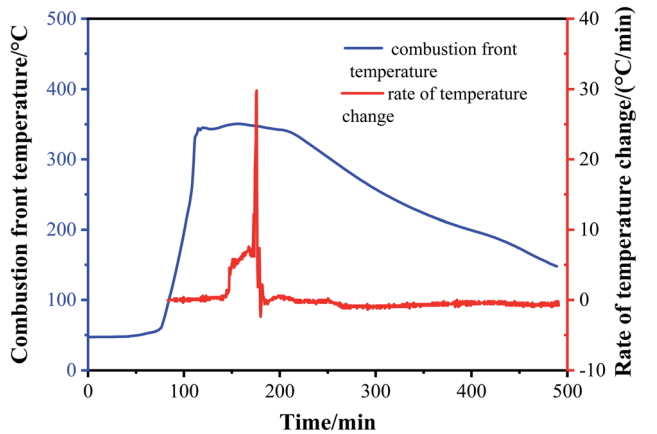

Fig. 4 Threshold temperature measurement of crude oil *in situ* combustion.

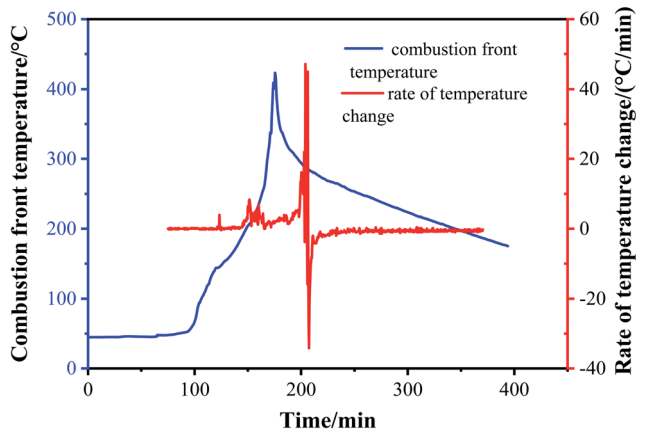

Fig. 5 Threshold temperature measurement of the residual oil *in situ* combustion after polymer flooding.

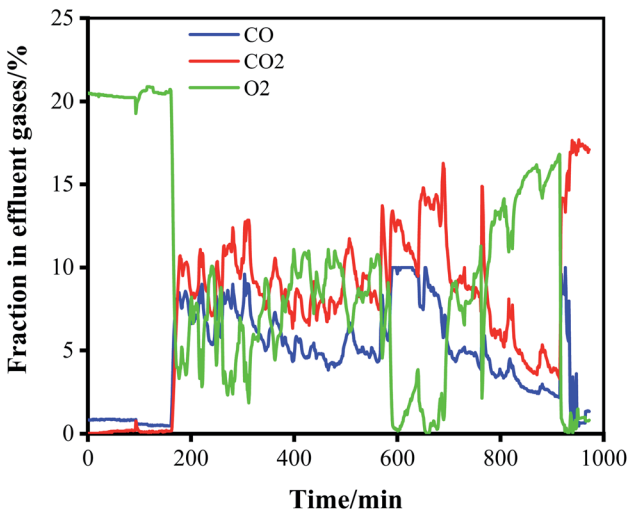

Fig. 6 Variation curve of effluent gas composition and time in crude oil ISC.

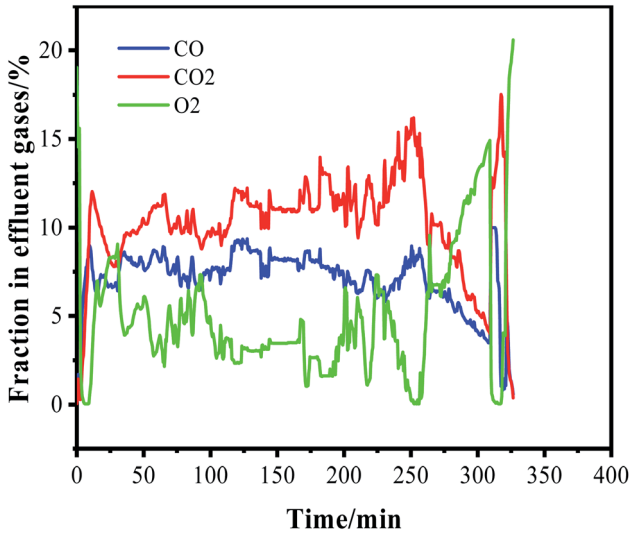

Fig. 7 Curve of effluent gas composition and time after polymer flooding in residual oil ISC.

stable advancement of the fire line, and the trend of the output effluent-gas component change is similar to that of the component change of the pure ISC experiment; therefore, the ISC technique can be implemented in the remaining oil reservoir after the polymer flooding.

Table 3 shows the basic parameters of the two groups of fire flooding experiments. The apparent H/C atomic ratio of the two groups of experiments is greater than 1 and less than 3, implying that their oxygen usage rate is greater than 85%, indicating that the high-temperature oxidation reaction dominates the fire flooding process. Compared with the experimental parameters of fire flooding, the fuel consumption of polymer flooding to fire flooding is lower, the air consumption, and stage air–oil ratio of polymer flooding to fire flooding are higher, and the fire line propulsion speed is similar. The oil displacement efficiency of polymer flooding to fire flooding is 72.1%, which is lower than 78.16% of the oil displacement efficiency of the fire flooding experiment. This is because the remaining oil after polymer flooding is more dispersed, with low saturation. Although the remaining oil consumes similar quality crude oil and has similar displacement ability in the low-temperature oxidation stage, less crude oil may be displaced by fire due to the lower initial oil saturation, resulting in low displacement efficiency. The remaining oil sands from the fire flooding were removed at the end of the experiment and the distribution of the oil sands after the fire flooding was observed; the oil sands after the fire flooding turned white, the chloroform asphalt measurement was performed, and the results showed that the remaining oil content saturation was close to 0. This implies that except for the displaced crude oil, the other crude oil is consumed by the combustion reaction, rather than remaining in the pores. The combustion reaction is sufficient and is unaffected by the residual formation water in the formation after polymer flooding, demonstrating the feasibility of the fire flooding experiment after dilute-oil polymer flooding.

3.2 Analysis of crude oil properties before and after fire flooding

3.2.1 Analysis of group composition. The determination of group components in oil samples was conducted according to the Chinese Petroleum and Natural Gas Industry Standard SY/T 5119-2008 "Column analysis method of rock-soluble organic matter and crude oil group components". Fig. 8 shows the measured results. The figure shows that the composition of crude oil changed significantly. Among them, the contents of asphaltene, saturated hydrocarbon, and aromatic hydrocarbon decreased from 3.99%, 59.38%, and 19.1% before the reaction

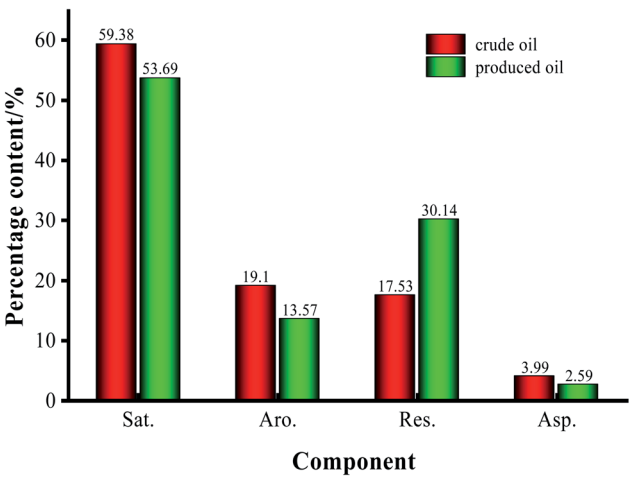

Fig. 8 Analysis of the crude oil group, composition properties of crude oil, and produced oil by residual oil fire flooding after polymer flooding.

Table 3 Basic parameters of residual oil after polymer flooding in residual oil by ISC

Serial number	Basic parameters of fire experiment	ISC	ISC after polymer flooding
1	H/C atomic ratio	1.16	1.33
2	Fuel consumption/(kg m^{-3})	24.72	23.10
3	Air consumption/L	246	260
4	Fuel consumption rate/%	21.84	27.90
5	Stage air-to-oil ratio AORs (m^3 t^{-1})	2825.29	4354.96
6	Fireline propulsion speed (cm h^{-1})	0.40	0.38
7	Oil-displacement efficiency/%	78.16	72.10

to 2.59%, 53.69%, and 13.57% after the reaction, respectively, and the contents of the resin increased significantly. Compared with crude oil before the reaction, the contents of asphaltene, saturated hydrocarbon, and aromatic hydrocarbon decreased by 1.4%, 5.69%, and 5.53%, whereas the content of rubber paper increased by 12.61%. The analysis shows that heavy components in crude oil are the primary source of fuel in the process of the burning oil layer. In this experiment, asphaltene, saturated hydrocarbons, and aromatic hydrocarbons were all reduced, indicating that the crude oil contains more long-chain or ring alkanes and polycyclic aromatic hydrocarbons. Coke is generated after high-temperature cracking and polymerization, and the decrease in the other three components increases the proportion of the resin.

3.2.2 Total hydrocarbon by gas chromatographic method analysis. Fig. 9(a) and (b) show the total hydrocarbon chromatogram analysis of crude oil and produced oil by residual oil fire flooding after polymer flooding, respectively. A comparison of the distribution of carbon number peaks in (a) and (b) reveals that the carbon number peaks of crude oil shifted forward and the highest peak was changed from C17 to C14 after the polymer flooding + fire flooding experiment. Table 4 shows that the contents of C10–C15 in the produced oil increase, whereas the content of C21 and subsequent carbon number hydrocarbons decrease significantly. The main components of the oxidation deposition into fuel are macromolecules, and the intermediate products of the fuel-deposition reaction process increase, indicating that the fuel deposition effect is good. This also shows that the fire flooding after polymer flooding can effectively reduce the heavy components in crude oil, advance the carbon number peak of an oil sample, and improve the crude oil quality.

Table 4 Total hydrocarbon table of crude oil and produced oil by residual oil fire flooding after polymer flooding by gas chromatographic method

Carbon distribution of hydrocarbons	Content/%	
	Crude oil	After polymer flooding + fire flooding produced oil
<C10	6.21	3.07
C10–C15	27.97	35.71
C16–C20	27.4	27.77
C21–C25	22.88	19.63
C26–C30	11.02	9.55
C31–C35	4.24	3.67
>C35	0.28	0.61

3.2.3 Infrared spectral analysis. In the infrared spectrum, 1600 cm^{-1} corresponds to the vibrational absorption peak of the C=C double bond of an aromatic skeleton, and 1700 cm^{-1} corresponds to the stretching vibrational absorption peak of the carbonyl group (C=O) in esters, ketones, and acid alcohols, and the change in absorption intensity at the 1700 cm^{-1} band is usually selected to correspond to the degree of crude oil oxidation. Fig. 10 shows that there is no absorption peak at 1700 cm^{-1} for crude oil, and the remaining oil after polymer flooding followed by fire flooding produced oil shows an obvious absorption peak at 1700 cm^{-1}, indicating that the fire flooding experiment of the remaining oil after polymer flooding can still maintain a high degree of oxidation. The ratio of A_{1700}

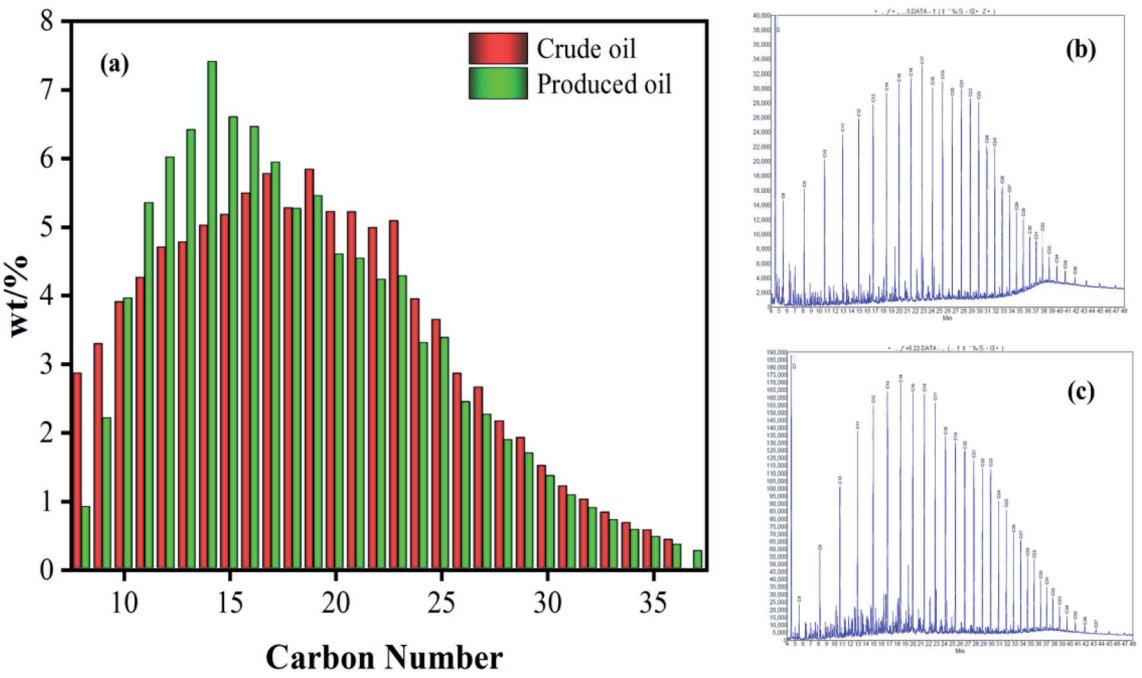

Fig. 9 Total hydrocarbon of crude oil and produced oil by the gas chromatographic method. (a) Carbon number distribution of crude oil and produced oil by residual oil fire flooding after polymer flooding. (b) Gas chromatogram of crude oil. (c) Gas chromatogram of produced oil.

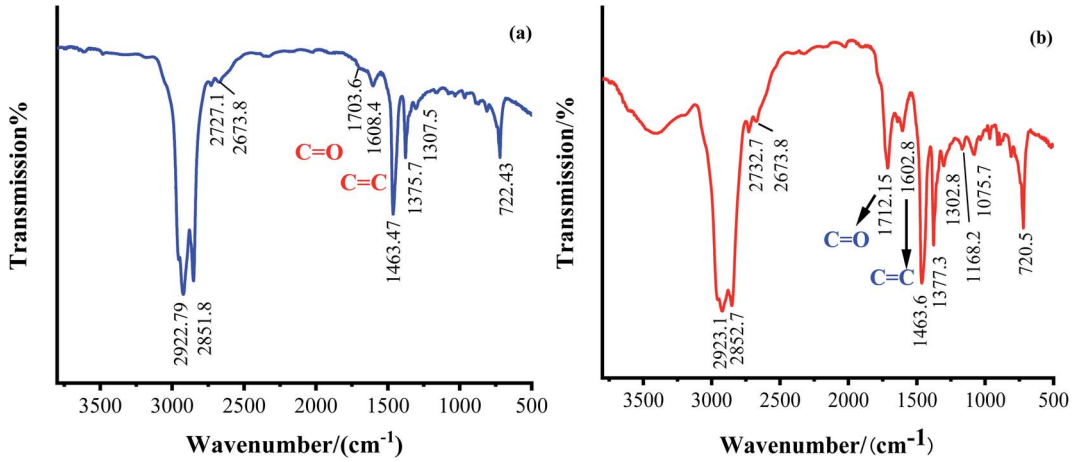

Fig. 10 FTIR transmittance spectra of the samples. (a) Infrared spectra of crude oil and (b) infrared spectra of produced oil.

to A_{1600} is used as the oxygen content (I_O) parameter in the infrared spectra, that is, the parameter in crude oil is 0.923, and that in output oil is 1.179.[11] This indicates that the oxidation reaction of crude oil is more intense during the fire flooding, and the combustion process is in the high-temperature oxidation stage, which generates functional groups with carbonyl groups, such as aldehydes, ketones, and carboxyl groups.

4 Conclusion

The experiment of fire flooding after polymer flooding was conducted in a one-dimensional combustion tube, and the following conclusions were drawn:

(1) The basic parameters of the fire flooding after the polymer flooding in the thin oil reservoir are examined using the temperature curve of the combustion front, the change curve of the tail gas, and the change in the crude oil composition before and after the fire flooding. The residual oil after the polymer flooding in the thin oil reservoir can still ignite and effectively and stably maintain the combustion state throughout the process. The combustion reaction is sufficient and the formation of residual water is unaffected by the polymer flooding.

(2) The remaining oil saturation after polymer flooding affects the threshold temperature of crude oil, fuel consumption, and other basic combustion parameters. The recovery efficiency of the burned oil layer is increased by 72.1% after polymer flooding, which is lower than that of direct crude oil by 78.16%. This is caused by low oil saturation, although fire flooding as a replacement technology for polymer flooding in thin oil reservoirs still has practical value.

(3) A comparison of the group composition and total hydrocarbon chromatogram of oil samples before and after burning oil layers reveals that after polymer flooding, the heavy components of produced oil decrease, light hydrocarbons increase, and the quality of crude oil improve. A comparison of the infrared spectra of oil samples before and after the reaction reveals that the residual oil after polymer flooding can still maintain a high degree of oxidation in the fire flooding experiment.

(4) This study is extremely useful for clarifying the feasibility of fire flooding in reservoirs after polymer flooding and investigating the influencing factors of reservoir changes on fire flooding effect after polymer flooding. It provides a significant experimental foundation and a high reference value for further research on fire flooding as a polymer flooding replacement technology for improving oil recovery in thin oil reservoirs.

Conflicts of interest

We declare that we have no financial and personal relationships with other people or organizations that can inappropriately influence our work, there is no professional or other personal interest of any nature or kind in any product, service and/or company that could be construed as influencing the position presented in, or the review of, the manuscript entitled "Feasibility study on further enhanced oil recovery by ISC of remaining oil after polymer flooding".

Acknowledgements

This work was supported by the National Science and Technology Major Projects of China for Oil and Gas (Projects No. 2016ZX05055 and 2016ZX05012).

References

1 J. X. Wang, G. R. Xu, Z. J. Fu, *et al.*, LTO laboratory experiments and reservoir selection criteria of air injection, *Pet. Geol. Recovery Effic.*, 2008, **15**(1), 69–71.
2 F. J. Zhao, Y. J. Liu, N. Lu, *et al.*, A review on upgrading and viscosity reduction of heavy oil and bitumen by underground catalytic cracking, *Energy Rep.*, 2021, **7**(10), 4249–4272.
3 Y. W. Jiang, Y. T. Zhang, S. Q. Liu, *et al.*, Mechanisms of oil drive for air injection development in low permeability reservoirs, *Pet. Explor. Dev.*, 2021, **37**(4), 471–476.
4 S. R. Ren, C. H. Yang, S. M. Hou, *et al.*, Exploration of the relationship between gas injection volume and air drive

mechanism in light reservoirs, *J. China Univ. Pet., Ed. Nat. Sci.*, 2012, **36**(3), 121–125.

5 H. B. Al-Saffar, H. Hasanin, D. Price, *et al.*, Oxidation Reactions of a Light Crude Oil and Its SARA Fractions in Consolidated Cores, *Energy Fuels*, 2001, **15**(1), 182–188.

6 Z. Wang, G. Liao, W. Pu, *et al.*, Oxidation reaction features of formation crude oil in air injection development, *Acta Pet. Sin.*, 2018, **39**(3), 314–319.

7 W. Pu, S. Zhao, L. Hu, *et al.*, Thermal effect caused by low temperature oxidation of heavy crude oil and its in situ combustion behavior, *J. Pet. Sci. Eng.*, 2019, **184**, 106521.

8 S. Bagci and M. V. Kok, In situ combustion laboratory studies of Turkish heavy oil reservoirs, *Fuel Process. Technol.*, 2001, **74**(2), 65–79.

9 J. P. Kisler and D. C. S. Member, An Improved Model for the Oxidation Processes of Light Crude Oil, *Chem. Eng. Res. Des.*, 1997, **75**(4), 392–400.

10 N. K. Gargar, A. A. Mailybaev, M. Dan, *et al.*, Effects of water on light oil recovery by air injection, *Fuel*, 2014, **137**, 200–210.

11 H. Q. Cheng, High-Temperature oxidation identification in fire-flooding, *Spec. Oil Gas Reservoirs*, 2018, **25**(128), 135–139.

12 H. Q. Cheng, Q. H. Zhao, B. L. Liu, *et al.*, Physical simulation research on basic parameters of in situ combustion for super heavy oil reservoirs, *Spec. Oil Gas Reservoirs*, 2012, **19**(4), 107–110.

13 R. G. Moore, S. A. Mehta and M. G. Ursenbach, *A guide to high pressure air injection (HPAI) based oil recovery. SPE75207*, 2002.

14 M. G. Ursenbach, R. G. Moore and S. A. Mehta, Air injection in heavy oil reservoirs-a process whose time has come(again), *J. Can. Pet. Technol.*, 2010, **49**(1), 48–54.

15 W. F. Pu, S. Zhao, J. J. Pan, *et al.*, Effect of low-temperature oxidation of light oil on oil recovery during high pressure air injection, *Pet. Sci. Technol.*, 2018, 1–7.

16 J. Li, S. A. Mehta, R. G. Moore, *et al.*, New insights into oxidation behaviours of crude oils, *J. Can. Pet. Technol.*, 2009, **48**(9), 12–15.

17 H. K. Sarma, N. Yazawan, R. G. Moore, *et al.*, Screening of three light-oil reservoirs for application of air injection process by accelerating rate calorimetric and TG/PDSC tests, *J. Can. Pet. Technol.*, 2002, **41**(3), 50–61.

18 Z. Chen, W. Lei, Q. Duan, *et al.*, High-Pressure Air Injection for Improved Oil Recovery: Low-Temperature Oxidation Models and Thermal Effect, *Energy Fuels*, 2013, **27**, 780–786.

19 J. Li, S. A. Mehta, R. G. Moore, *et al.*, Investigation of the oxidation behavior of pure hydrocarbon components and crude oils utilizing PDSC thermal technique, *J. Can. Pet. Technol.*, 2006, **45**(1), 48–53.

20 H. Jia, J. Z. Zhao, W. F. Pu, *et al.*, Thermal study on light crude oil for application of high-Pressure air injection (HPAI) process by TG/DTG and DTA tests, *Energy Fuels*, 2012, **26**(3), 1575–1584.

21 S. Huang, Y. Zhang and J. J. Sheng, Experimental Investigation of Enhanced Oil Recovery Mechanisms of Air Injection under a Low-Temperature Oxidation Process: Thermal Effect and Residual Oil Recovery Efficiency, *Energy Fuels*, 2018, **32**(6), 6774–6781.

22 C. Clara, M. Durandeau, G. Quenault, *et al.*, Laboratory studies for light-oil air injection projects:potential application in handily field, *SPE Reservoir Eval. Eng.*, 2000, **3**(3), 239–248.

23 T. Teramoto, H. Uematsu, K. Takabayashi and T. Onishi, *Air injection EOR in highly water saturated light-oil reservoir. SPE100215*, 2006.

24 Z. Xu, Y. L. Jian and T. S. Liang, Research on the mechanisms of enhancing recovery of light-oil reservoir by air-injected low-temperature oxidation technique, *Nat. Gas Ind.*, 2004, **24**(4), 78–80.

25 A. Askarova, E. Popov, M. Ursenbach, *et al.*, Experimental Investigations of Forward and Reverse Combustion for Increasing Oil Recovery of a Real Oil Field, *Energies*, 2020, **13**(17), 4581.

26 Y. Liu, F. J. Zhao, Y. X. Wu, *et al.*, Study on the application of a steam-foam drive profile modification technology for heavy oil reservoir development, *Open Chem.*, 2021, **19**(1), 678–685.

27 R. B. Zhao, Y. G. Wei, Z. M. Wang, *et al.*, Kinetics of Low-Temperature Oxidation of Light Crude Oil, *Energy Fuels*, 2016, **30**(4), 2647–2654.

28 Z. Y. Chen, B. L. Niu, L. Z. Tang, *et al.*, Experimental study of low temperature oxidation mechanism and activity of oil components, *J. Fuel Chem. Technol.*, 2013, **41**(11), 1336–1342.